Formation of Digallium Sites in the Reaction of Trimethylgallium with Silica

Ziyad A. Taha,[†] Eric W. Deguns,[‡] Swarup Chattopadhyay,[†] and Susannah L. Scott*[,†,‡]

Department of Chemical Engineering and Department of Chemistry and Biochemistry, University of California, Santa Barbara, California 93106-5080

Received December 3, 2005

The room-temperature, gas−solid reaction of volatile $GaMe_3$ with a nonporous silica was studied by elemental and gas-phase analysis, in situ IR and ^1H, ^{13}C, and ^{29}Si solid-state NMR, and extended X-ray absorption fine structure (EXAFS) spectroscopy. Most of the grafting (∼85%) occurred on Q^3 sites, O_3SiOH, but a small amount (∼15%) of siloxane ($O_3SiO-SiO_3$) bond cleavage was also observed. The major, if not the only, gallium product has the empirical formula ≡$SiOGaMe_2$, but it is not an "isolated" site. The Ga K-edge EXAFS of $GaMe_3$-modified silica, recorded at 10 K, reveals that each Ga has a Ga neighbor at 2.97−2.99 Å. The sites are best described as $[GaMe_2(\mu\text{-}OSi\equiv)]_2$. To strengthen this assignment, a molecular analogue, $[GaMe_2(\mu\text{-}OSiPh_3)]_2$, was characterized by both single-crystal X-ray diffraction and EXAFS. The Ga_2O_2 rings in the molecular complex and the silica-supported gallium dimer have very similar dimensions. The gallium dimer is formed on the silica surface regardless of the extent of partial dehydroxylation (varied by pretreatment in vacuo at 100 and 500 °C). This result is interpreted in terms of a vicinal disposition for the majority of Q^3 grafting sites.

Introduction

Gallosilicates catalyze the dehydrogenation[1,2] and aromatization[3,4] of alkanes and the selective reduction of nitrogen oxides by hydrocarbons.[5] A gallosilicate catalyst is used in the BP-UOP Cyclar process, by which liquefied petroleum gas (LPG, primarily propane and butane) is converted to BTX (benzene/toluene/xylene).[6] The catalytic activity and selectivity depend on the extent of dispersion of the gallium in the silicate framework. High dispersion may be achieved by grafting a volatile molecular precursor onto the surface. $GaMe_3$ has been used in this way to prepare gallosilicate catalysts,[7−11] in which the resulting Ga sites were assumed to be isolated.

$GaMe_3$ adsorbs reversibly on silica at cryogenic temperatures.[12] Above 273 K, it reacts with the surface hydroxyl groups, liberating methane.[12−14] The proposed reaction is shown in eq 1,

$$\equiv SiOH + GaMe_3 \rightarrow \equiv SiOGaMe_2 + MeH \qquad (1)$$

where ≡SiOH denotes a sterically accessible Q^3 site on the silica surface. In previous studies, the gallium product was formulated as a three-coordinate dimethylgallium(III) fragment, with a trigonal coordination environment similar to that of $GaMe_3$ both in the gas phase[15] and in solution.[16] The hydrolytic stability of the methyl ligands in $GaMe_3/SiO_2$ led one group to propose extensive grafting of $GaMe_3$ onto siloxane bridges (eq 2), generating unreactive Si−C bonds,[13]

$$\equiv SiOSi\equiv + GaMe_3 \rightarrow \equiv SiOGaMe_2 + \equiv SiMe \qquad (2)$$

where ≡SiOSi≡ represents a pair of vicinal Q^4 sites and ≡SiMe is a T^1 site (monomethylated silicon atom). This hypothesis was refuted in a subsequent investigation, although a minor contribution from reaction 2 could not be ruled out.[14] Grafting reactions analogous to eqs 1 and 2 have long been proposed for $AlMe_3$, whose deposition on silica can be used to create Lewis acid sites that activate metallocene catalysts for olefin polymerization.[17] These grafted sites have been described in many studies as three-coordinate ≡$SiOAlMe_2$ and $(\equiv SiO)_2AlMe$.[18−22] However, we recently concluded that $AlMe_3$ reacts

* To whom correspondence should be addressed. E-mail: sscott@engineering.ucsb.edu. Fax: 1-805-893-4731.
[†] Department of Chemical Engineering.
[‡] Department of Chemistry and Biochemistry.

(1) Giannetto, G.; Montes, A.; Gnep, N. S.; Florentino, A.; Cartraud, P.; Guisnet, M. *J. Catal.* **1993**, *145*, 86−95.
(2) Mériaudeau, P.; Sapaly, G.; Naccache, C. *J. Mol. Catal.* **1993**, *81*, 293−300.
(3) Thomas, J. M.; Liu, X.-S. *J. Phys. Chem.* **1986**, *90*, 4843−4847.
(4) Choudhary, V. R.; Devadas, P.; Kinage, A. K.; Sivadinarayana, C.; Guisnet, M. *J. Catal.* **1996**, *158*, 537−550.
(5) Pushkar, Y. N.; Sinitsky, A.; Parenago, O. O.; Kharlanov, A. N.; Lunnia, E. V. *Appl. Surf. Sci.* **2000**, *167*, 69−78.
(6) Mowry, J. R.; Anderson, R. F.; Johnson, J. A. *Oil Gas J.* **1985**, *83*, 1288−1293.
(7) Bayense, C. R.; van Hooff, J. H. C.; de Haan, J. W.; van de Ven, L. J. M.; Kentgens, A. P. M. *Catal. Lett.* **1993**, *17*, 349−361.
(8) Seidel, U.; Koch, M.; Brunner, E.; Staudte, B.; Pfeifer, H. *Micropor. Mesopor. Mater.* **2000**, *35*−*36*, 341−347.
(9) García-Sánchez, M.; Magusin, P. C. M. M.; Hensen, E. J. M.; Thüne, P. C.; Rozanska, X.; van Santen, R. A. *J. Catal.* **2005**, *219*, 352−361.
(10) Hensen, E. J. M.; García-Sánchez, M.; Rane, N.; Magusin, P. C. M. M.; Liu, P.-H.; Chao, K.-J.; van Santen, R. A. *Catal. Lett.* **2005**, *101*, 79−85.
(11) Kazansky, V. B.; Subbotina, I. R.; van Santen, R. A.; Hensen, E. J. M. *J. Catal.* **2005**, *233*, 351−358.
(12) Mawhinney, D. B.; Glass, J. A.; Yates Jr., J. T. *J. Vac. Sci. Technol. A* **1999**, *17*, 679−685.
(13) Tubis, R.; Hamlett, B.; Lester, R.; Newman, C. G.; Ring, M. A. *Inorg. Chem.* **1979**, *18*, 3275−3276.
(14) Morrow, B. A.; McFarlane, R. A. *J. Phys. Chem.* **1986**, *90*, 3192−3197.
(15) Beagley, B.; Schmidling, D. G.; Steer, I. A. *J. Mol. Struct.* **1974**, *21*, 437−444.
(16) Muller, N.; Otermat, A. L. *Inorg. Chem.* **1965**, *4*, 296−299.
(17) Chien, J. C. W. *Top. Catal.* **1999**, *7*, 23−36.
(18) Peglar, R. J.; Hambleton, F. H.; Hockey, J. A. *J. Catal.* **1971**, *20*, 309−320.
(19) Morrow, B. A.; Hardin, A. H. *J. Phys. Chem.* **1979**, *83*, 3135−3141.
(20) Bartram, M. E.; Michalske, T. A.; Rogers, J. W. *J. Phys. Chem.* **1991**, *95*, 4453−4463.

10.1021/om051034o CCC: $33.50
Publication on Web 03/18/2006

with the surface of a fumed silica to give four-coordinate dialuminum surface sites, on the basis of the reaction stoichiometry.[23]

The organometallic chemistry of trivalent aluminum is similar to that of gallium in many ways, including a proclivity for four-coordination with heteroatom-donor ligands. The persistence of undercoordinated metal (Al, Ga) sites on silica, despite the abundance and proximity of potential oxygen donors, is therefore unexpected. Coordination numbers have been evaluated for hydrated alumino- and gallosilicates by their NMR chemical shifts;[24,25] however, both ^{27}Al and ^{71}Ga exhibit very broad, frequently undetectable NMR resonances in the solid state under the strictly anhydrous conditions required to prevent decomposition of their organometallic compounds.[8,9,23] Furthermore, the presence of water is likely to alter the metal coordination number, since it binds strongly to Lewis acid sites.

We undertook an investigation of the reaction of $GaMe_3$ with silica in an effort to elucidate the structures of grafted group III sites. Elemental analysis and IR, ^{1}H, ^{29}Si, and ^{13}C solid-state NMR, and extended X-ray absorption fine structure (EXAFS) spectroscopy were employed. In particular, EXAFS was used to probe the local environment of gallium. The technique is indifferent to the degree of long-range order and is thus well-suited to the study of structure in amorphous materials, such as oxide-supported metal complexes. While the EXAFS of Al is complicated by the need for UHV conditions at the low X-ray energy of the Al K-edge (1.5596 keV), as well as strong interference from the overlapping K-edge of Si (1.8389 keV), the Ga K-edge (10.3671 keV) is more accessible, and high-quality spectra of gallosilicate materials are readily obtained.[26,27]

Experimental Section

Materials and Reagents. The silica used in this work is Aerosil 380 (denoted A380), a nonporous, pyrogenic silica from Degussa, with a BET surface area of (340 ± 2) m^2/g and an average primary particle size of 7 nm. The thermal pretreatment temperature of the silica is indicated by its appended number. For example, A380−500 indicates a sample of A380 treated at 500 °C. A standard pretreatment procedure was followed in order to ensure reproducibility. A380−500 was prepared by calcining the silica under 300 Torr of O_2 at 500 °C for at least 3 h. The silica was then partially dehydroxylated at 500 °C for at least 4 h under dynamic vacuum (<10^{-4} Torr). To prepare silica at a lower dehydroxylation temperature, the calcination step was omitted. The silica was simply heated to the appropriate temperature for 4 h under dynamic vacuum. These thermal treatments do not alter the surface area of the silica, but they do standardize the number of surface hydroxyl groups.

$GaMe_3$ (colorless liquid) was purchased from Aldrich and transferred in the glovebox into an all-glass reactor sealed with two high-vacuum Teflon stopcocks (Young valves) arranged in series. *Caution! Neat $GaMe_3$ is pyrophoric. Handle only small (<1 mL) quantities outside the glovebox, and dispose of unreacted material by controlled alcoholysis in a fume hood.* Water was double-distilled and then transferred into a high-vacuum glass reactor equipped with a glass stopcock greased with Apiezon-H (Varian). Before use, each liquid reagent was subjected to several freeze−pump−thaw cycles in order to remove dissolved gases and then introduced into the experimental reactor via gas-phase transfer through a high-vacuum manifold (<10^{-4} Torr). In general, an excess of $GaMe_3$ was sublimed at room temperature and condensed onto the silica with the aid of a liquid-N_2 bath. After the mixture was warmed to room temperature, the reaction of $GaMe_3$ with silica was allowed to proceed under vacuum, in the absence of solvent or inert gases, for 20 min. Volatiles, including physisorbed $GaMe_3$, were desorbed at room temperature to a liquid nitrogen trap.

IR Spectroscopy. Experiments were performed in an in situ IR cell, equipped with a high-vacuum stopcock and either KCl or ZnSe windows affixed to the Pyrex body with TorrSeal (Varian). Silica was pressed at 40 kg/cm^2 into a self-supporting disk 1.6 cm in diameter, containing ca. 15 mg of silica. A thinner film was prepared by spreading silica onto a ZnSe window, to increase the transparency below 1300 cm^{-1}. Transmission infrared spectra were recorded on a Shimadzu PrestigeIR spectrometer equipped with a DTGS detector and purged with CO_2-free dry air. Background and sample spectra were recorded by co-adding 32 scans at a resolution of 2 cm^{-1}.

Solid-State NMR Spectroscopy. For NMR experiments, 50−100 mg of silica was compacted into thick pellets and then coarsely ground in a mortar. ^{1}H, ^{13}C, and ^{29}Si solid-state NMR spectra were recorded on a Bruker ASX-300 spectrometer. Samples were loaded into 4 mm zirconia rotors in an Ar-filled glovebox equipped with O_2 and moisture sensors. ^{1}H MAS NMR spectra were recorded at 300.05 MHz. The spectra were collected using a 2 μs 45° pulse, a relaxation delay of 0.2 s, and an acquisition time of 49 ms. ^{13}C and ^{29}Si CP-MAS NMR spectra were recorded at frequencies of 75.46 and 56.62 MHz, respectively. ^{13}C spectra were collected using a contact time of 2 ms and a relaxation delay of 2 s. ^{29}Si spectra were collected using a contact time of 10 ms and a relaxation delay of 1 s. All samples were spun at 10 kHz. Water, adamantane, and tetrakis(trimethylsilyl)silane were used as external chemical shift references for ^{1}H, ^{13}C, and ^{29}Si, respectively. ^{13}C and ^{29}Si spectra were baseline-corrected and treated with 50 Hz line broadening.

^{71}Ga MAS NMR spectroscopy was attempted on a Bruker DMX500 spectrometer, using a 1.6 μs 90° pulse, a relaxation delay of 2 s, and an acquisition time of 4.2 ms. The sample was spun at 14 kHz.

Mass Balance. Methane was quantified in situ by IR spectroscopy. A calibration curve in the range 5−30 Torr was constructed using the intensity of the CH_4 deformation mode at 1306 cm^{-1}. At the end of each experiment, the $GaMe_3$-modified silica was weighed in air and then stirred overnight in 1.67 M HNO_3 containing 35% aqueous H_2O_2 (0.1 mL/mL of sample solution). The solution was filtered and its gallium content analyzed by ICP. A calibration curve was constructed by diluting an atomic absorption standard solution (998 ppm of Ga, Fluka).

Synthesis and Single-Crystal X-ray Diffraction of [$GaMe_2$-(μ-$OSiPh_3$)]$_2$. The model complex was synthesized using Schlenk techniques under a dry nitrogen atmosphere. Solvents were rigorously dried and deaerated prior to use by passage over molecular sieves and activated alumina. To 4.6 g (0.017 mol) of Ph_3SiOH in 40 mL of toluene at room temperature was added a solution of 1.9 g of $GaMe_3$ (0.017 mol) in 20 mL of toluene with stirring. Immediate evolution of methane gas was observed. After the mixture was stirred for 24 h, toluene was removed in vacuo (ca. 100 mTorr) to give [$GaMe_2$(μ-$OSiPh_3$)]$_2$ as a white powder. Recrystallization from a mixture of hexane and benzene afforded a crystalline solid. Yield: ca. 70%. Solution NMR spectra were

(21) Anwander, R.; Palm, C.; Groeger, O.; Engelhardt, G. *Organometallics* **1998**, *17*, 2027−2036.
(22) Puurunen, R. C.; Root, A.; Sarv, P.; Viitanen, M. M.; Brongersma, H. H.; Lindblad, M.; Krause, A. O. I. *Chem. Mater.* **2002**, *14*, 720−729.
(23) Scott, S. L.; Church, T. L.; Nguyen, D. H.; Mader, E. A.; Moran, J. *Top. Catal.* **2005**, *34*, 109−120.
(24) Bayense, C. R.; Kentgens, A. P. M.; de Haan, J. W.; van de Ven, L. J. M.; van Hooff, J. H. C. *J. Phys. Chem.* **1992**, *96*, 775−782.
(25) McManus, J.; Ashbrook, S. E.; MacKenzie, K. J. D.; Wimperis, S. *J. Non-Cryst. Solids* **2001**, *282*, 278−290.
(26) Meitzner, G. D.; Iglesia, E.; Baumgartner, J. E.; Huang, E. S. *J. Catal.* **1993**, *140*, 209−225.
(27) Nishi, K.; Shimizu, K.; Takamatsu, M.; Yoshida, H.; Satsuma, A.; Tanaka, T.; Yoshida, S.; Hattori, T. *J. Phys. Chem. B* **1998**, *102*, 10190−10195.

recorded on a Bruker DPX200 spectrometer. ^{1}H NMR ($CDCl_3$, δ): 7.15−7.50 (m, 30H, Ph); −0.53 (s, 12H, GaMe). $^{13}C\{^1H\}$ NMR ($CDCl_3$, δ): −2.12 (GaMe); 127.75 (s, 12 C, *m*-C phenyl); 130.07 (s, 6 C, *p*-C phenyl); 135.08 (s, 12 C, *o*-C phenyl); 135.75 (C_6H_5) (s, 6 C, Si−C phenyl). Elemental analysis was performed under N_2. Anal. Calcd for $C_{40}H_{42}Ga_2O_2Si_2$: C, 64.03; H, 5.64. Found: C, 63.55; H, 5.54.

A diffraction-quality single crystal of $[GaMe_2(\mu\text{-}OSiPh_3)]_2$ was grown by slow diffusion of hexane into a benzene solution of the compound under N_2. A colorless crystal of approximate dimensions 0.20 × 0.15 × 0.08 mm was mounted on a glass fiber and transferred to a Bruker CCD platform diffractometer. Data collection (20 s/frame, 0.3°/frame for a sphere of diffraction data) and determination of unit cell parameters were accomplished using the program SMART.[28] The data were collected at 120 K, using an Oxford nitrogen gas cryostream system. Raw frame data were processed using the program SAINT.[29] Subsequent calculations were carried out using the program SHELXTL.[30] The structure was solved by direct methods and refined on F^2 by full-matrix least-squares techniques. All non-hydrogen atoms were refined anisotropically. Hydrogen atoms were located from difference Fourier synthesis and refined isotropically.

X-ray Absorption Spectroscopy. Spectra at the Ga K-edge (10.3671 keV) were recorded on beamline 2-3 (Bend) at the Stanford Synchrotron Radiation Laboratory (SSRL), operated at 3.0 GeV with a ring current of 80−100 mA. X-rays were monochromatized via reflection from a pair of Si(111) crystals, through a 1 mm entrance slit. The incident beam was detuned 50% to suppress harmonics. Samples were mounted at 45° to the beam, to collect transmission and fluorescence spectra simultaneously. The intensity of the incident beam was measured with a N_2-filled ion chamber detector installed in front of the sample. Transmitted X-rays were detected in a second, Ar-filled ion chamber. Fluorescence from the sample was recorded at right angles to the beam, using an Ar-purged Lytle detector without Soller slits.

The highly air-sensitive sample powders were packed under a dry N_2 atmosphere into aluminum plates with slots 10 × 4 × 2 mm, between windows of 12 μm polypropylene film (Chemplex #475) affixed with double-sided tape to each side of the plate. To avoid spectral artifacts due to thickness effects, $[GaMe_2(\mu\text{-}OSiPh_3)]_2$ was diluted with BN to ca. 10 wt % Ga. $GaMe_3/SiO_2$ samples did not require dilution. Spectra were recorded at 10 K in an Oxford Instruments liquid He flow cryostat. Three data sweeps (total collection time ~1 h) were averaged to improve the signal-to-noise ratio. Fluorescence data were generally of better spectral quality than transmission data and were therefore used in data analysis.

EXAFS Data Analysis. Data processing and analysis were performed using WinXAS (version 3.1).[31,32] XAS spectra were background-corrected by subtracting a linear fit to the preedge region extrapolated to the length of the entire spectrum and then normalized by a seventh-degree polynomial fitted to the postedge region. EXAFS spectra were k^3-weighted and fitted by a polynomial spline with 6 knots between 1.5 and 14.5 Å^{-1}. A Bessel window ($\alpha = 4$) was applied to the data before Fourier transformation to R space. The data were fitted to single-scattering paths using the EXAFS equation (eq 3) with least-squares refinement.[33] N_i is the number of scatterers in the ith shell at a distance R from the absorber. The Debye−Waller factor, σ_i^2, is the root-mean-squared relative displacement of these scatterers, $\lambda(k)$ is the mean-free path of the photoelectron, and $\phi(k)_i$ and $F(k)_i$ are the phase shift and backscattering amplitude, respectively. The phase shift and backscattering amplitude functions were calculated using FEFF 8.20.[34,35]

$$\chi(k) = S_0^2 \sum_i \frac{N_i F_i(k)}{kR_i^2} \exp(-2k^2\sigma_i^2) \exp\left(\frac{-2R_i}{\lambda(k)}\right) \sin(2kR_i + \phi_i(k)) \quad (3)$$

Table 1. Stoichiometries (mmol/g of silica)[a] for $GaMe_3$ Uptake on Silica and Subsequent Hydrolysis of Grafted $GaMe_3/SiO_2$

	$GaMe_3$/A380-500		$GaMe_3$/A380-100	
	grafting	hydrolysis	grafting	hydrolysis
Ga uptake	1.04 ± 0.04 (6)		1.55 ± 0.09 (7)	
MeH	0.88 ± 0.04 (9)	1.96 ± 0.07 (4)	1.35 ± 0.05 (8)	2.84 ± 0.10 (5)
≡SiMe[b]	0.16 ± 0.06	0.12 ± 0.08	0.20 ± 0.10	0.26 ± 0.07

[a] Reported as means and standard deviations; numbers in parentheses represent the number of independent experiments. [b] Calculated as the difference between the expected and observed methane yields (expected: 1.0 MeH/Ga for grafting and 2.0 MeH/Ga for hydrolysis).

Results and Discussion

Grafting Stoichiometry. When excess $GaMe_3$ was sublimed onto A380-500 and allowed to react at room temperature, a portion of the organometallic complex chemisorbed on the silica surface. The only volatile product detected by gas-phase IR spectroscopy was methane: 0.88 ± 0.04 mmol/g of silica. The amount of methane is equivalent to the number of accessible hydroxyls on this silica.[36] Analysis of the $GaMe_3$-modified silica after desorption of unreacted $GaMe_3$ revealed the presence of 6.75 ± 0.28 wt % Ga, or 0.95 ± 0.04 mmol of Ga/g of sample. After correction for the mass gained during grafting (9.7 wt % for the $GaMe_2(-H)$ fragment), the Ga uptake was therefore 1.04 ± 0.04 mmol of Ga/g of silica. Quantitative results are summarized in Table 1.

The ratio of evolved methane per chemisorbed Ga suggests that a grafting reaction such as eq 1 therefore represents the fate of 85 ± 5% of $GaMe_3$. The difference between the Ga uptake, 1.04 mmol/g of silica, and the methane yield upon grafting, 0.88 mmol/g of silica, is attributed to a minor reaction (15 ± 6%) of $GaMe_3$ with siloxane bonds (eq 2). It contributes 0.16 ± 0.06 mmol of ≡SiMe/g of silica. A mass balance was sought by quantifying the methyl groups liberated as methane upon exhaustive hydrolysis of the $GaMe_3$-modified silica. Only a trace of methane was detected upon addition of excess water vapor at room temperature. This is consistent with the well-known stability of dimethylgallium(III) fragments to protonolysis.[14,37,38] However, after the material was heated to 200 °C for 3 h, 1.96 ± 0.07 mmol of MeH/g of silica was evolved, corresponding to 1.88 MeH/Ga. If all gallium sites can be described by the same empirical formula, $\equiv SiOGaMe_2$, regardless of their grafting origin via reactions such as eqs 1 and 2, this result suggests that a very small amount of additional

(28) SMART, version 5.1; Bruker Advanced X-ray Solutions, Inc., Madison, WI, 1999.
(29) SAINT, version 5.1; Bruker Advanced X-ray Solutions, Inc., Madison, WI, 1999.
(30) Sheldrick, G. M. SHELXTL, version 6.12; Bruker Advanced X-ray Solutions, Inc.: Madison, WI, 2001.
(31) Ressler, T. *J. Phys. IV* **1997**, *7*, 269−270.
(32) Ressler, T.; Wong, J.; Roos, J. *J. Synchroton Radiat.* **1999**, *6*, 656−658.
(33) Sayers, D. E.; Stern, E. A.; Lytle, F. W. *Phys. Rev. Lett.* **1971**, *27*, 1204−1207.
(34) Ankudinov, A. L.; Ravel, B.; Rehr, J. J.; Conradson, S. D. *Phys. Rev. B* **1998**, *58*, 7565.
(35) Ankudinov, A. L.; Bouldin, C.; Rehr, J. J.; Sims, J.; Hung, H. *Phys. Rev. B* **2002**, *65*, 104107−11.
(36) Taha, Z. A. Ph.D. Thesis, University of Ottawa, 2004.
(37) Beachley, O. T.; Kirss, R. U.; Bianchini, R. J.; Royster, T. L. *Organometallics* **1987**, *6*, 724−727.
(38) Chesnut, R. W.; Cesati, R. R.; Cutler, C. S.; Pluth, S. L.; Katzenellenbogen, J. A. *Organometallics* **1998**, *17*, 4889−4896.

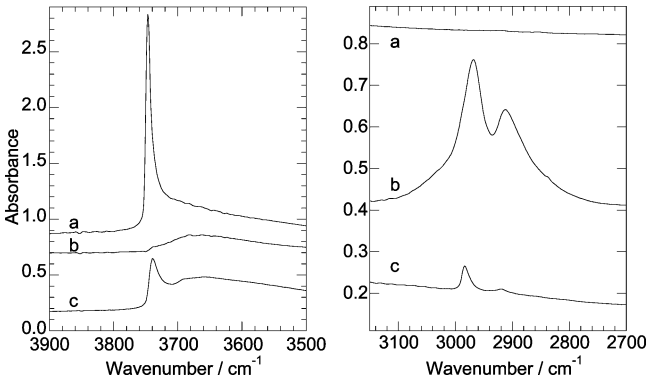

Figure 1. Room-temperature IR spectra of A380 silica (a) after thermal pretreatment at 500 °C, (b) after reaction with excess $GaMe_3$, and (c) after exposure of the $GaMe_3$-modified silica to excess water vapor at 200 °C, in the ν(O−H) and ν(C−H) regions. All spectra were recorded under vacuum, after removal of volatiles, and are vertically offset for clarity.

≡SiMe (0.12 ± 0.08 mmol/g) was formed at the elevated temperature required to effect hydrolysis.

Similar results were obtained at a lower silica pretreatment temperature, corresponding to a higher initial density of surface hydroxyl groups (but no adsorbed water). The methane yield upon reaction of A380-100 with excess $GaMe_3$ was 1.35 ± 0.05 mmol/g of silica. This is consistent with a population of accessible hydroxyls that is ca. 45% greater on Aerosil pretreated at 100 °C compared to 500 °C.[36] The material contained 9.66 ± 0.57 wt % Ga, or 1.36 ± 0.08 mmol of Ga/g of sample. Adjusting for the mass gained upon grafting (13.7 wt % for the $GaMe_2$(−H) fragment), the Ga uptake was 1.55 ± 0.09 mmol/g of silica. The difference between the amount of chemisorbed Ga, 1.55 mmol/g of silica, and the methane yield upon grafting, 1.35 mmol/g of silica, is again attributed to the reaction of $GaMe_3$ with siloxane bonds (13 ± 6%), producing 0.20 ± 0.10 mmol of ≡SiMe/g of silica. Thus, the ratio of grafting pathways (silanol vs siloxane) does not depend on the silica pretreatment temperature. Exhaustive hydrolysis with excess water vapor at 200 °C resulted in liberation of 2.84 ± 0.10 mmol of MeH/g of silica, corresponding to 1.83 ± 0.07 MeH/Ga. The missing methane is again ascribed to the formation of ≡SiMe during hydrolysis (0.26 ± 0.07 mmol/g of silica).

Infrared Characterization. Infrared spectra of a self-supporting disk of A380-500, before and after its reaction with $GaMe_3$, are shown in Figure 1. The sharp band at 3747 cm^{-1} due to the stretching mode ν(SiO−H) of the isolated surface hydroxyl sites of silica disappears almost completely during the reaction. Only a weak, broad absorption band remains, centered at approximately 3665 cm^{-1} (Figure 1b). It is assigned to internal silanols, perturbed by the silica matrix,[39] that are unreactive toward $GaMe_3$[14] and many other inorganic hydrogen-sequestering agents, including $AlMe_3$, $TiCl_4$, and $VOCl_3$.[23,40] They are therefore described as inaccessible silanols. The IR evidence suggests that the accessible hydroxyl groups of silica are completely consumed by reaction with excess $GaMe_3$ at room temperature.

After evacuation of volatiles (i.e., methane and unreacted $GaMe_3$), two new bands were observed in the ν(C−H) region at 2968 and 2914 cm^{-1} (Figure 1b). They are assigned to the asymmetric and symmetric stretching modes, respectively, of methyl groups bonded to Ga, by comparison to the gas-phase IR spectrum of $GaMe_3$ (2961 and 2911 cm^{-1}).[41] The methyl deformation mode $\delta_{as}(CH_3)$ appeared at 1420 cm^{-1}, while $\delta_s(CH_3)$ was obscured by the intensely absorbing lattice modes of the silica below 1300 cm^{-1}. However, by using spectral subtraction to remove contributions from silica lattice modes, its overtone $2\delta_s(CH_3)$ was detected at 2407 cm^{-1}. IR bands below 1300 cm^{-1} were observed by preparing a thin film of the silica supported on a ZnSe window (see Figure S1 in the Supporting Information). All assignments are summarized in Table S1; they are consistent with those reported by Morrow and McFarlane,[14] who demonstrated that the attributions of an earlier study[13] to ≡SiMe vibrations were in error.

Virtually identical IR spectra were recorded using Aerosil A300-100 (Figure S2, Supporting Information), except that the stretching modes of unreacted surface hydroxyls after treatment of the silica with excess $GaMe_3$ were more intense. This is consistent with a report that the fraction of inaccessible hydroxyl groups is greater on A380-100 than on A380-500.[39]

When $GaMe_3$-modified silica was exposed to excess water vapor at room temperature, the stretching vibration of the ≡SiO−H groups at 3747 cm^{-1} did not reappear, and only a trace of methane was observed in the gas phase. When the sample was heated at 200 °C in the presence of adsorbed water for 2 h, a large amount of methane was observed in the gas phase, and almost all of the intensity attributed to methyl vibrations disappeared. A sharp band at 3743 cm^{-1} appeared, accompanied by a broad band centered at 3670 cm^{-1} (Figure 1c). The former is assigned to regenerated silica silanols. The latter may contain contributions from perturbed silanols as well as ν(GaO−H) stretching modes, since its frequency is similar to that reported for the hydroxyl-terminated surface of Ga_2O_3.[42]

After hydrolysis, two very small peaks remained in the C−H stretching region, at 2983 and 2925 cm^{-1}. They are assigned to the asymmetric and symmetric methyl stretching modes of ≡SiMe sites.[14,43] Assuming that the extinction coefficients for the stretching vibrations of different types of methyl groups are similar, integration of the absorbance in the ν(C−H) region before and after hydrolysis allows the fraction of the original methyl groups present as non-hydrolyzable ≡SiMe to be estimated at ∼5%.

Solid-State NMR. The ^{1}H MAS NMR spectrum of $GaMe_3$-modified A380−500 (Figure 2a) consists of a broad signal with a maximum at −1.0 ppm. This peak is assigned to Ga−CH_3 and is shielded relative to the corresponding signals in the molecular analogues $[Ga(CH_3)_2(\mu\text{-}OSiPh_3)]_2$, −0.55 ppm, and $\{[(c\text{-}C_5H_9)_7Si_7O_{11}(OSiMePh)_2)]_2(Ga(CH_3)_2)_4\}$, −0.20 ppm.[44] The signal for Si−CH_3 sites is expected to appear in the same region; however, it was not resolved until after hydrolysis (see below). The ^{13}C CP-MAS NMR spectrum of the same sample is shown in Figure 3a. A peak at −4.4 ppm is assigned to Ga−CH_3, also shielded relative to the signals for $[Ga(CH_3)_2(\mu\text{-}OSiPh_3)]_2$, −2.12 ppm, and $\{[(c\text{-}C_5H_9)_7Si_7O_{11}(OSiMePh)_2)]_2(Ga(CH_3)_2)_4\}$, −1.91 ppm.[44] A shoulder at ca. −7 ppm is tentatively assigned to ≡SiCH_3 sites. For comparison, a chemical shift of −5.2 ppm was reported for monomethylated T^1 sites $(SiO)_3SiCH_3$ on silica.[45]

(39) Morrow, B. A.; McFarlan, A. J. *Langmuir* **1991**, *7*, 1695−1701.
(40) Rice, G. L.; Scott, S. L. *Langmuir* **1991**, *7*, 1695−1701.
(41) Kvisle, S.; Rytter, E. *Spectrochim. Acta, Part A* **1984**, *40A*, 939−951.
(42) Vimont, A.; Lavalley, J. C.; Sahibed-Dine, A.; Otero Areán, C.; Rodríguez Delgado, M.; Daturi, M. *J. Phys. Chem. B* **2005**, *109*, 9656−9664.
(43) Morrow, B. A.; McFarlan, A. J. *J. Non-Cryst. Sol.* **1990**, *120*, 61−71.
(44) Gerritsen, G.; Duchateau, R.; van Santen, R. A.; Yap, G. P. A. *Organometallics* **2003**, *22*, 100−110.
(45) Tao, T.; Maciel, G. E. *J. Am. Chem. Soc.* **2000**, *122*, 3118−3126.

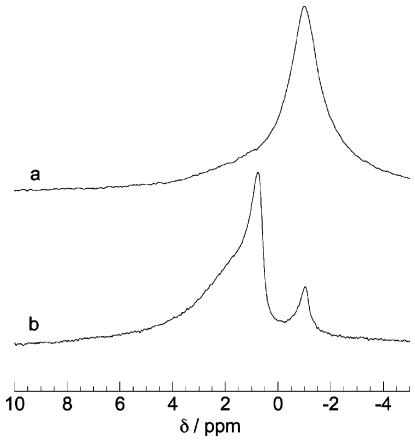

Figure 2. ^{1}H MAS NMR spectra of (a) $GaMe_3$-modified A380-500 and (b) the sample in (a) after exposure to water vapor at 200 °C, followed by evacuation at the same temperature.

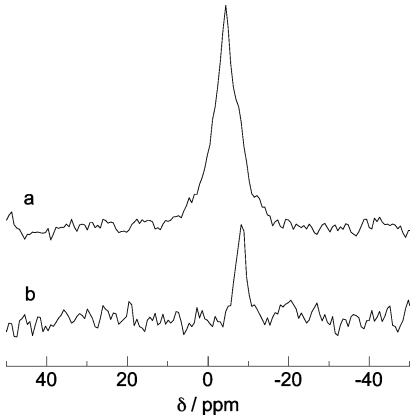

Figure 3. ^{13}C CP-MAS NMR spectra of (a) $GaMe_3$-modified A380-500 and (b) the sample in (a) after exposure to water vapor at 200 °C, followed by evacuation at the same temperature.

Addition of water vapor to $GaMe_3$-modified A380-500 and heating at 200 °C for 2 h followed by evacuation at the same temperature resulted in a dramatic decrease in the ^{1}H NMR signal intensity at −1.0 ppm and the appearance of a new signal at +0.7 ppm (Figure 2b). The latter is assigned to Ga(*μ*-O*H*)-Ga, by comparison to the chemical shift of 0.77 ppm reported for [^{t}Bu$_2$Ga(*μ*-OH)]$_3$.[46,47] The ≡SiO*H* signal appeared as a broad shoulder centered at 2 ppm.[48] The persistence of a small signal at −1.0 ppm is consistent with the presence of ≡Si*C*H$_3$ sites that are stable toward hydrolysis.[49] In the ^{13}C CP-MAS NMR spectrum of the same sample, the signal at −4.4 ppm completely disappeared, exposing a small peak at −8.1 ppm (Figure 3b). It is assigned to nonhydrolyzable ≡Si*C*H$_3$ sites on the surface.

The ^{29}Si CP-MAS NMR spectrum of $GaMe_3$-modified A380−500 shows a broad signal at −106 ppm assigned to both (SiO)$_4$*Si* and (SiO)$_3$(GaO)*Si* sites (Figure 4a). The resonance at −60 ppm is assigned to ≡*Si*Me. For comparison, a chemical shift of −62 ppm was reported for T^1 sites on silicas treated with a variety of methylating agents.[45] After hydrolysis, the peak centered at −105 ppm appears narrower and more intense

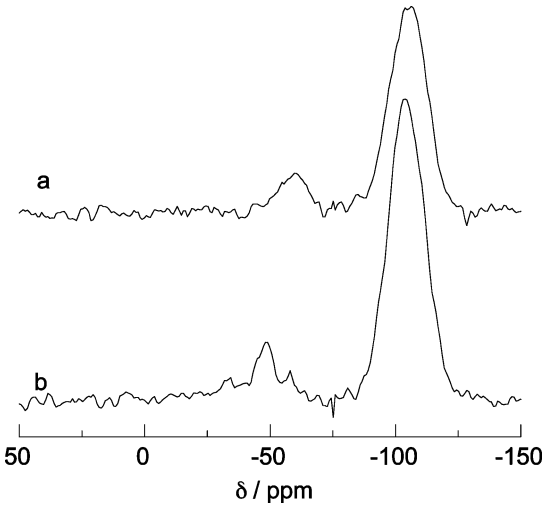

Figure 4. ^{29}Si CP-MAS NMR spectra of (a) $GaMe_3$-modified A380-500 and (b) the sample in (a) after exposure to water vapor at 200 °C, followed by evacuation at 200 °C.

Chart 1. Structures Considered for Silica-Supported $GaMe_3$, Consistent with the Empirical Formula ≡SiOGaMe$_2$

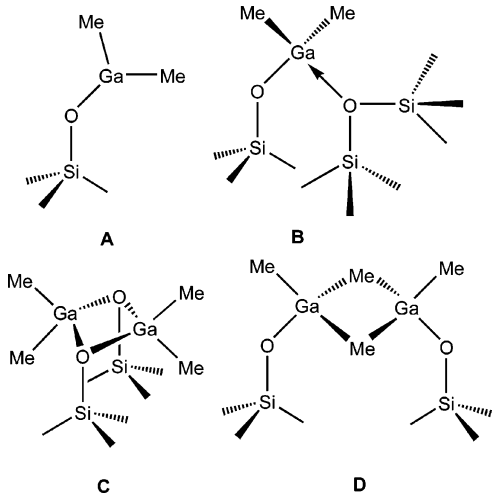

(Figure 4b), presumably due to the contribution of more efficiently cross-polarized Q^3 sites (SiO)$_3$*Si*OH formed by the hydrolytic cleavage of SiOGa linkages.[50] The ≡SiMe signal shifts downfield, to −49 ppm. Its new position suggests that it corresponds to (≡SiO)$_2$*Si*(OH)(Me) sites, for which a chemical shift of −52 ppm has been reported.[45] Thus, the nonhydrolyzable Si−C bonds are found in sites that also possess a gallium neighbor, (≡SiO)$_2$(GaO)*Si*Me, to which the prehydrolysis peak at −60 ppm is attributed.

No ^{71}Ga signal was detected for the unhydrolyzed sample under MAS conditions, even after 48 h of acquisition. This absence of signal intensity is attributed to locally distorted Ga environments, resulting in large quadrupolar coupling constants. Similar negative results have been reported previously for other $GaMe_3$-modified oxide materials.[7,9]

EXAFS Analysis of $GaMe_3$-Modified Silica. Several structures consistent with the empirical formula of the gallium sites, ≡SiOGaMe$_2$, are shown in Chart 1. Model **A** was proposed in previous studies of the reaction between $GaMe_3$ and amorphous silica and a zeolite.[10,13,14] Molecular organogallium(III) alkoxides and siloxides are well-known to aggregate, or to form adducts with Lewis bases, to render gallium four-coordinate.[44,51−54] The

(46) Naiini, A. A.; Yong, V.; Han, Y.; Akinc, M.; Verkade, J. G. *Inorg. Chem.* **1993**, *32*, 3781−3782.
(47) Storre, J.; Klemp, A.; Roesky, H. W.; Schmidt, H.-G.; Noltemyer, R.; Fleischer, R.; Stalke, D. *J. Am. Chem. Soc.* **1996**, *118*, 1380−1386.
(48) Bronnimann, C. E.; Zeigler, R. C.; Maciel, G. E. *J. Am. Chem. Soc.* **1988**, *110*, 2023−2026.
(49) Uhl, W.; Hannemann, F. *J. Organomet. Chem.* **1999**, *579*, 18−23.
(50) Haukka, S.; Root, A. *J. Phys. Chem.* **1994**, *98*, 1695−1703.

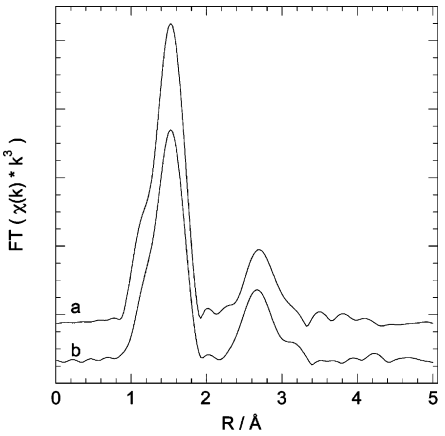

Figure 5. Fourier transform magnitude EXAFS in non-phase-corrected *R* space for (a) $GaMe_3$-modified A380-100 and (b) $GaMe_3$-modified A380-500, at the Ga K-edge. The spectra are vertically offset for clarity.

predominance of electron-deficient three-coordinate Ga centers on silica (model **A**) therefore seems unlikely. Coordination of a neighboring siloxane oxygen is represented in model **B**. However, the considerably more electron-rich siloxane oxygens of silsesquioxanes do not coordinate to dimethylgallium(III) siloxides; instead, dimeric structures with bridging siloxide ligands are formed.[55] A silica analogue, with bridging siloxides derived from the hydroxyl groups of the silica surface, is shown in model **C**. If the spatial distribution of surface hydroxyls on silica is not conducive to the formation of **C**, a digallium structure may be formed with bridging methyl ligands, **D**. Evidence for the presence of one or more of these structures was sought using EXAFS.

The k^3-weighted Fourier-transformed EXAFS spectra for $GaMe_3$-modified A380-100 and A380-500 silicas, recorded at 10 K, look very similar (Figure 5), suggesting that the same sites dominate on both surfaces. The proposed models shown in Chart 1 were evaluated by curve-fitting these spectra. For each model, the coordination numbers were fixed at integer values and interatomic distances were constrained to be >1.8 Å.[56] The goodness of fit was evaluated by the magnitude of the residual and, more importantly, the plausibility of the fitted bond distances and Debye−Waller factors.

When model **A** was refined to the data, the Debye−Waller factor for its Ga−O path ($N = 1$) was $\sigma^2 = -9.6 \times 10^{-4}$ Å^2 (see Table S2, Supporting Information). Since negative thermal disorder is not possible, this result suggests that a first coordination sphere consisting of only one O and two C neighbors cannot generate enough intensity for the peak at 1.6 Å in *R* space. Including a second, independent Ga−O path (i.e., model **B**) generated physically meaningful values for all Debye−Waller factors (see Table S3). This model accounts for the first coordination sphere of Ga (i.e., C_2O_2) but provides no intensity for the peak at 2.7 Å.

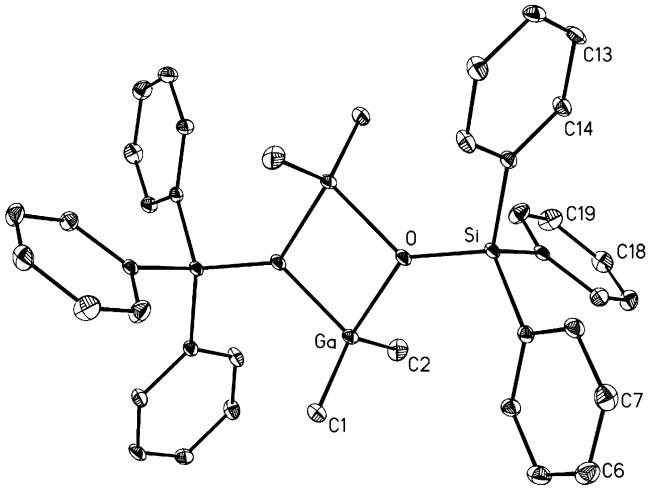

Figure 6. Structure of $[Me_2Ga(\mu\text{-}OSiPh_3)]_2$. Thermal ellipsoids are drawn at the 30% probability level. Hydrogen atoms are omitted for clarity. Selected bond lengths (Å): C(1)−Ga, 1.953(4); C(2)−Ga, 1.943(3); Ga−O#1, 1.976(2); Ga−O, 1.9800(19); Ga−Ga#1, 2.9813(7); O−Si, 1.656(2). Selected angles (deg): C(2)−Ga−C(1), 127.50(18); C(2)−Ga−O#1, 110.95(14); C(1)−Ga−O#1, 109.76(13); C(2)−Ga−O, 105.85(12); C(1)−Ga−O#1, 111.23(13); O#1−Ga−O, 82.21(8).

Table 2. Crystal Data for $[(GaMe_2)(\mu\text{-}OSiPh_3)]_2$

formula	$C_{20}H_{21}GaOSi$
fw	375.18
cryst syst	triclinic
space group	$P\bar{1}$
a, Å	8.7861(11)
b, Å	9.5628(12)
c, Å	12.8261(16)
α, deg	69.910(2)
β, deg	74.453(2)
γ, deg	64.222(2)
V, Å^3	902.3(2)
Z	2
μ(Mo Kα), mm^{-1}	1.593
cryst size, mm	0.2 × 0.15 × 0.08
total no. of data points	6534
no. of unique data points	3886
GOF	1.058
R1, wR2 ($I > 2\sigma(I)$)	0.0402, 0.1098

In a recent XAS study of $GaMe_3$ adsorbed in ZSM-5,[9] a peak at $R = 2.9$ Å was assumed to arise from a Si or Al backscatterer of the zeolite support, although no curve fitting of this path was attempted. Modifying model **B** to include a Si atom at this distance caused the Debye−Waller factor expand to an unrealistically large value (~0.04 Å^2). However, the presence of a Ga backscatterer (i.e., model **C**) resulted in a good fit to both the imaginary component and the FT magnitude. Our hypothesis that the EXAFS contains a Ga−Ga path led us to synthesize a molecular dimer of dimethylgallium and to analyze its EXAFS under similar conditions.

X-ray Diffraction Study and X-ray Absorption Spectroscopy of $[GaMe_2(\mu\text{-}OSiPh_3)]_2$. Although $[GaMe_2(\mu\text{-}OSiPh_3)]_2$ has been previously reported[57] and its dimeric nature inferred by measurement of its molecular weight, structural parameters were not determined. It was synthesized by the reaction of equivalent amounts of Ph_3SiOH and $GaMe_3$. The results of single-crystal X-ray diffraction are shown in Figure 6. Crystal data and details of the structure refinement are reported in Table 2. The molecule consists of two identical $GaMe_2$ fragments bridged by two triphenylsiloxide ligands, such that the geometry

(51) Schmidbaur, H. *Angew. Chem., Int. Ed. Engl.* **1965**, *3*, 201−211.
(52) Murugavel, R.; Voigt, A.; Walawalkar, M. G.; Roesky, H. W. *Chem. Rev.* **1996**, *96*, 2205−2236.
(53) Keys, A.; Barbarich, T. J.; Bott, S. G.; Barron, A. R. *Dalton Trans.* **2000**, 577−588.
(54) Oliver, J. G.; Worrall, I. J. *J. Chem. Soc. A* **1970**, 845−848.
(55) Duchateau, R.; Dijkstra, T. W.; van Santen, R. A.; Yap, G. P. A. *Chem. Eur. J.* **2004**, *10*, 3979−3990.
(56) Constraining the bond distances to ≥1.8 Å was necessary because of a low-*R* shoulder on the first maximum in *R* space, possibly due to incomplete background removal of the atomic XAFS. Without this constraint, path lengths for some scatterers in the first coordination sphere of Ga were refined to physically implausible values: i.e., $R < 1.7$ Å.
(57) Schmidbaur, H.; Schindler, F. *Chem. Ber.* **1966**, *99*, 2178−2186.

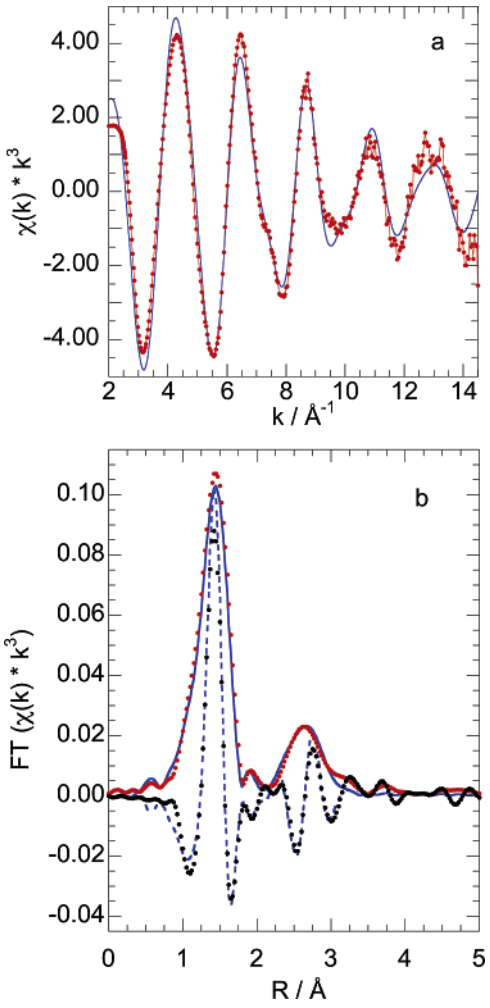

Figure 7. Ga K-edge EXAFS for $[GaMe_2(\mu\text{-}OSiPh_3)]_2$ in k^3-weighted k space (top; red line) and non-phase-corrected R space (bottom; imaginary data given as black points and FT magnitude as red points). The curve fit to the single-scattering model based on the crystal structure is shown (blue line).

at gallium is distorted tetrahedral. The Ga−C distances, at 1.943(3) and 1.953(4) Å, are comparable to the average distance reported for the oligomeric silsesquioxane analogue $\{[(c\text{-}C_5H_9)_7Si_7O_{11}(OSiMePh_2)]_2(GaMe_2)_4\}$, 1.947 Å.[39] The Ga−Ga nonbonded distance of 2.98 Å is close to that reported for $[(c\text{-}C_5H_9)_7Si_7O_{10}(OSiPh_2O)(GaMe_2)]_2$, at 2.99 Å.[55] The bridging triphenylsiloxide ligands are almost symmetrically disposed between the two gallium atoms, with Ga−O and Ga−O#1 distances of 1.9800(19) and 1.976(2) Å, respectively. These distances, as well as the C−Ga−C and O−Ga−O bond angles, are also comparable to those previously observed for dimethylgallium(III) with silsequioxane ligands.[44,55] Only the Si−O distance, at 1.656(2) Å, is slightly longer than that reported for the silsesquioxane complexes, 1.617(3) Å. This is likely a consequence of the different silicon coordination environments.

The EXAFS of $[GaMe_2(\mu\text{-}OSiPh_3)]_2$ was recorded at the Ga K-edge at 10 K, to directly compare EXAFS-derived structural parameters with those obtained by single-crystal X-ray diffraction. The EXAFS spectrum is shown in Figure 7. Its resemblance to the spectrum of $GaMe_3$-modified silica, including the prominent peak at 2.7 Å, is striking. The model used in curve fitting was constructed from the crystallographic parameters for $[GaMe_2(\mu\text{-}OSiPh_3)]_2$. Coordination numbers were fixed at integer values, while bond distances were constrained to vary by no more than ±0.15 Å. All other parameters in the fit (σ^2, ΔE_0 and S_0^2) were allowed to refine freely. The curve fit is shown in both k^3-weighted k space and R space in Figure 7. The same fitted parameters were obtained when the fit was performed with either k^3- or k^1-weighted data. Path lengths for the single-scattering model containing one C shell ($N = 2$), one O shell ($N = 2$), and one Ga shell ($N = 1$) are compared with the bond distances obtained by X-ray diffraction in Table 3. The agreement is well within the experimental uncertainty of the EXAFS technique, validating our curve-fitting approach. Allowing either the Ga−C or Ga−O paths (each with $N = 2$) to be refined independently (i.e., as two shells with $N = 1$) returned the same distances for each type of scatterer (within 0.01 Å). When the coordination numbers were also refined, their fitted values were within 10% of the required integers (N is strongly correlated with σ^2).

Table 3. Comparison of Bond Distances Obtained by Single-Crystal X-ray Diffraction and EXAFS Curve Fitting[a] for $[(GaMe_2)(\mu\text{-}OSiPh_3)]_2$

	XRD	EXAFS[b]			
path	R (Å)	N	R (Å)	σ^2 (Å^2)	ΔE_0 (eV)
Ga−C	1.943, 1.953	2	1.94	0.0027	2.01
Ga−O	1.976, 1.980	2	1.99	0.0070	1.15
Ga−Ga	2.981	1	2.98	0.0079	1.12
Ga−Si	3.294, 3.303				

[a] Errors for single-scattering fits, in the absence of systematic fitting uncertainties, are generally to be accepted as follows: bond lengths, ±0.02 Å; σ^2, ±20%; ΔE_0, ±20%. [b] $S_0^2 = 0.74$; residual 6.6.

The model described above generates no intensity for the shoulder apparent in R space at 3.1 Å. Due to the phase correction, this feature may represent a backscatter at 3.3−3.4 Å. We attempted to refine the Ga−Si path ($N = 2$) by fixing the Ga−Si distance at its crystallographic value, 3.30 Å. However, the associated value of σ^2 increased to >0.04 Å^2 (Table S4, Supporting Information). This result implies that a Ga−Si path does not contribute significantly to the EXAFS. We also investigated whether the feature at 3.1 Å could arise from a multiple scattering path (Ga−O−Ga, Ga−O−O, or Ga−C−O). However, inclusion of any combination of these paths was not justified by a statistically significant improvement in the fit.

Structure of $GaMe_3$-Modified Silica. The EXAFS of $GaMe_3$ supported on A380-100 and A380-500 was analyzed by curve fitting to the same single-scattering model used to fit the EXAFS of $[GaMe_2(\mu\text{-}OSiPh_3)]_2$. The results are shown for A380-500 in Figure 8; parameters obtained from the fits are reported in Table 4. The fitted values of the Ga−C and Ga−O paths and their associated Debye−Waller factors are very similar to those obtained for the molecular complex, and the inner-potential shifts ΔE_0 are all small, <|1.2| eV. The peak at 2.7 Å is generated by the Ga backscatterer. When the coordination numbers were refined, values close to the expected integers were again found (2.2, 1.9, and 1.0 for C, O, and Ga shells, respectively; see Table S5, Supporting Information), suggesting that the sites are highly uniform. We were again unable to refine a Ga−Si path to the EXAFS data. Silicon is often reported to be a weak EXAFS backscatterer, and our previous attempts to locate Si-containing paths for silica-supported metal complexes were unsuccessful.[58] Inclusion of multiple-scattering paths to the refinement yielded no statistically significant results.

Finally, the fitted Ga−C path lengths are not compatible with a digallium surface complex bridged by methyl ligands, model

(58) Deguns, E. W.; Taha, Z.; Meitzner, G. W.; Scott, S. L. *J. Phys. Chem. B* **2005**, *109*, 5005−5011.

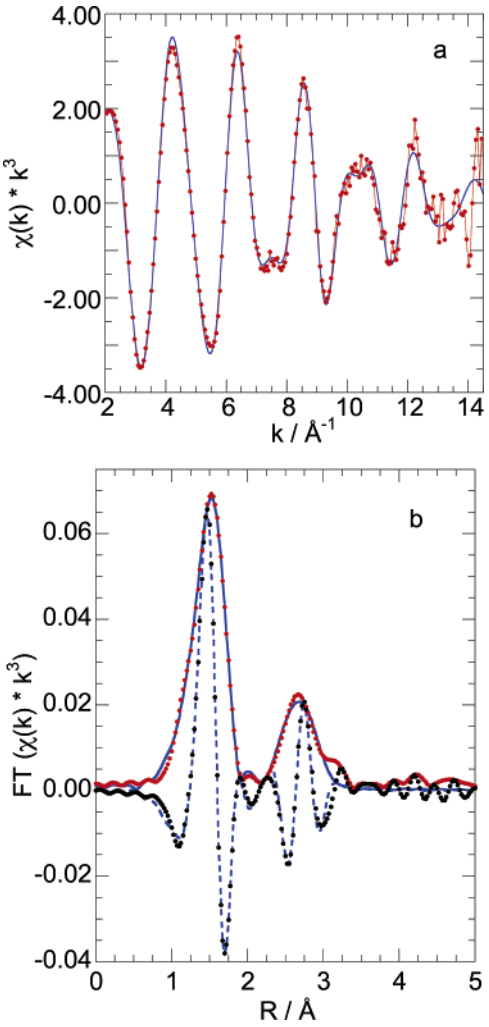

Figure 8. Ga K-edge EXAFS for $GaMe_3$-modified A380-500 in k^3-weighted k space (top; red line) and non-phase-corrected R-space (bottom; imaginary data given as black points and FT magnitude as red points). The curve fit to the single-scattering model for $[GaMe_2(\mu\text{-OSi}\equiv)]_2$ is shown (blue line).

Table 4. EXAFS Parameters for Single-Scattering Paths in Model C, $[(GaMe_2)(\mu\text{-OSi}\equiv)]_2$, Fitted to Data Obtained for $GaMe_3$-Modified A380-100 and A380-500[a]

	$GaMe_3$/A380-100[b]				$GaMe_3$/A380-500[c]			
path	N^d	R (Å)	σ^2 (Å^2)	ΔE_0 (eV)	N^d	R (Å)	σ^2 (Å^2)	ΔE_0 (eV)
Ga−C	2	1.95	0.0045	0.65	2	1.95	0.0032	1.19
Ga−O	2	1.98	0.0071	−0.35	2	1.98	0.0089	−0.88
Ga−Ga	1	2.99	0.0090	1.06	1	2.97	0.0088	0.70

[a] Errors for single-scattering fits, in the absence of systematic fitting uncertainties, are generally to be accepted as follows: bond lengths, ±0.02 Å; σ^2, ±20%; ΔE_0, ±20%. [b] $S_0^2 = 0.78$; residual 6.1. [c] $S_0^2 = 0.78$; residual 6.6. [d] Coordination numbers were fixed at integer values during fit refinement.

D. Examples of molecular complexes of Ga containing bridging methyls are rare, and $GaMe_3$ itself shows little tendency to dimerize.[16] However, in heterobimetallic complexes containing $Me_2Ga(\mu\text{-Me})_nM$ (M = Zr, Nd, La; n = 1, 2), the $Ga-C_{bridging}$ distances (2.033−2.142 Å) are always significantly longer than the $Ga-C_{terminal}$ distances (1.968−1.984 Å).[59,60] For $GaMe_3$/SiO_2, the fitted Ga−C path length of 1.95 Å is consistent with terminal methyl ligands. In sum, the EXAFS supports a siloxide-bridged dimethylgallium dimer (model **C** in Scheme 1) for the structure of $GaMe_3$-modified A380 silica at 10 K.

Curve fitting of the EXAFS of $GaMe_3$-modified A380-100 (Figure S7, Supporting Information) gave fit parameters identical with those obtained for A380-500, within experimental uncertainty (Table 4). Thus, the coordination environment of Ga is independent of the initial hydroxyl density of the silica. The Debye−Waller factors for the Ga−Ga paths in both silica-supported samples are the same, 0.009 Å^2, and the Debye−Waller factor for the same path in $[GaMe_2(\mu\text{-OSiPh}_3)]_2$ is very similar (0.008 Å^2). This result requires that the Ga_2O_2 rings in all three materials be of similar size and flexibility, even though the orientation of the bridging "siloxide" ligand substituents is trans in the molecular silanolate but is presumably cis for the silica-supported complexes.

The simplest explanation for the uniformity of the grafted sites is that the reactive hydroxyls are disposed vicinally on the silica surface, regardless of the average hydroxyl density. Such a spatial arrangement is consistent with reports of the reactions of metal alkyls MR_4 on silicas partially dehydroxylated at ≤200 °C.[61−65] It is plausible that such sites persist on silica partially dehydroxylated at 500 °C, since vicinal Q^3 sites in amorphous silicas are unable to form intramolecular hydrogen bonds,[66] nor do they condense to form four-membered siloxane rings at temperatures below 650 °C.[67] Vicinal sites are indistinguishable from truly isolated Q^3 sites by either IR or ^{29}Si NMR spectroscopy.

A proposed mechanism for the major grafting reaction, consistent with that originally envisaged in eq 1 but revised to incorporate vicinal Q^3 sites, is shown in Scheme 1. Reaction with $GaMe_3$ yields the digallium site **I**. Grafting of $GaMe_3$ on a small fraction of isolated Q^3 sites is proposed to give the less stable $(\equiv SiO)_3SiOGaMe_2$, site **II**, which may interact with an adjacent siloxane oxygen. Since the fitted coordination number N for the Ga−Ga path was found to be 0.96 (Table S5), we propose that site **II** spontaneously promotes the cleavage of an adjacent siloxane bond by $GaMe_3$ to give the digallium site **III** and a methylated silicon. The amount of silicon methylation observed during grafting (Table 1) allows us to estimate the ratio of vicinal to isolated Q^3 sites to be 6.8 ± 2.4 on A380-100 and 4.5 ± 1.7 on A380-500.

The driving force for siloxane cleavage is presumably the strong preference of gallium to achieve four-coordination through bridging siloxide ligands, rather than through either bridging methyl or siloxane ligands. Ga-induced siloxane cleavage has precedent in the reaction of the dimer of *tert*-butoxygallane with tetraphenyl-1,3-disiloxanediol: one of the gallosiloxane products is a result of ring expansion to give a $[GaO_4Si_3]_2$ framework.[68] Finally, hydrolysis of the Ga−O bonds of site **III** accounts for the formation of $(\equiv SiO)_2MeSiOH$, which

(59) Erker, G.; Albrecht, M.; Krüger, C.; Werner, S. *J. Am. Chem. Soc.* **1992**, *114*, 8531−8536.
(60) Evans, W. J.; Anwander, R.; Doedens, R. J.; Ziller, J. W. *Angew. Chem., Int. Ed. Engl.* **1994**, *33*, 1641−1644.
(61) Ballard, D. G. H. *Adv. Catal.* **1973**, *23*, 263−325.
(62) Candlin, J. P.; Thomas, H. *Adv. Chem. Ser.* **1974**, *No. 132*, 212−239.
(63) Yermakov, Y.; Zakharov, V. *Adv. Catal.* **1975**, *24*, 173-219.
(64) Schwartz, J.; Ward, M. D. *J. Mol. Catal.* **1980**, *8*, 465−469.
(65) Amor Nait Ajjou, J.; Scott, S. L. *Organometallics* **1997**, *16*, 86−92.
(66) Bunker, B. C.; Haaland, D. M.; Michalske, T. A.; Smith, W. L. *Surf. Sci.* **1989**, *222*, 95−118.
(67) Morrow, B. A.; Cody, I. A. *J. Phys. Chem.* **1976**, *80*, 1998−2004.
(68) Veith, M.; Vogelgesang, H.; Huch, V. *Organometallics* **2002**, *21*, 380−388.

Scheme 1. Proposed Grafting Mechanism for $GaMe_3$ on Vicinal and Isolated Q^3 Hydroxyl Sites on the Silica Surface

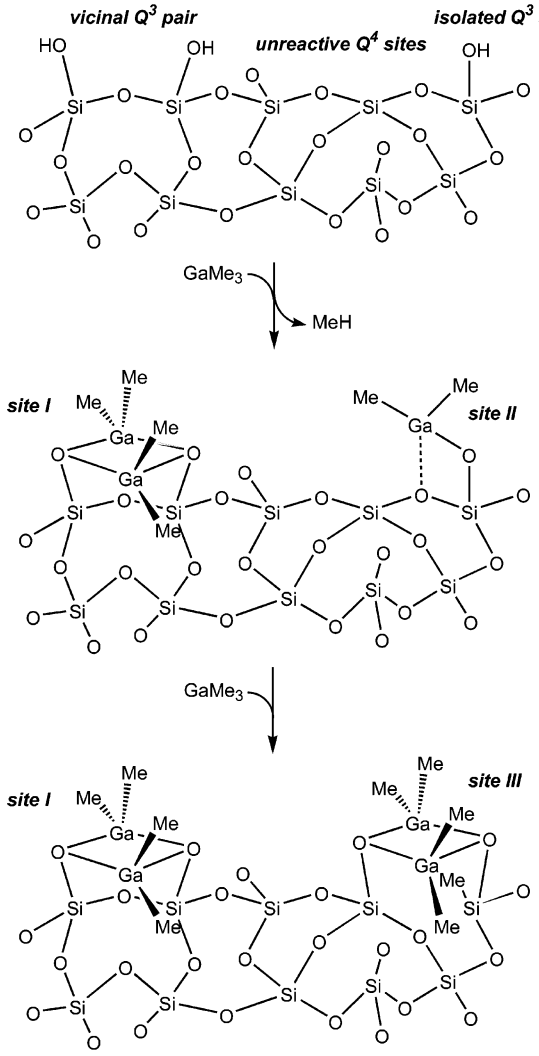

causes the shift in the ^{29}Si CP-MAS signal from −60 to −49 ppm.

Conclusions

The reactions of $GaMe_3$ with the surface of a fumed silica, partially dehydroxylated at either 100 or 500 °C, results in grafted sites with the empirical formula $\equiv SiOGaMe_2$. Two reaction pathways were inferred. The major pathway involves the reaction of $GaMe_3$ with vicinal surface hydroxyl groups. A minor pathway involves grafting of $GaMe_3$ onto isolated hydroxyl groups, followed by reaction with a second equivalent of $GaMe_3$ via siloxane cleavage. The EXAFS of the $GaMe_3$-modified silicas contains clear evidence for a well-defined Ga−Ga scattering path, identified as a rigid Ga_2O_2 ring by comparison to the EXAFS of $[GaMe_2(\mu\text{-}OSiPh_3)]_2$. All of the digallium fragments are formulated as $[GaMe_2(\mu\text{-}OSi\equiv)]_2$, tethered by two bridging siloxide ligands to the silica surface. The mechanisms of transformations of these digallium sites (e.g., to supported gallium chlorides or hydrides by treatment with HCl or H_2, respectively)[7,10,11,13] and their subsequent catalytic activity, previously assumed to be noninteracting monogallium sites, will need to be reinterpreted in this light. Finally, considering the similarities in $GaMe_3$ and $AlMe_3$ chemistry, it seems likely that the latter will also react to form four-coordinate dialuminum sites on silica.[23]

Acknowledgment. This work was funded in part by the U.S. Department of Energy, Basic Energy Sciences, Catalysis Science (Grant No. DE-FG02-03ER15467). Portions of this research were carried out at the Stanford Synchrotron Radiation Laboratory, a national user facility operated by Stanford University on behalf of the U.S. Department of Energy, Office of Basic Energy Sciences. This work also made use of MRL Central Facilities supported by the MRSEC Program of the National Science Foundation under Award No. DMR00-80034.

Supporting Information Available: Tables and figures giving additional IR spectra and EXAFS curve fits and a CIF files giving crystallographic data for $[Me_2Ga(\mu\text{-}OSiPh_3)]_2$. This material is available free of charge via the Internet at http://pubs.acs.org.

OM051034O